

# Isentropic perturbations of a chaotic domain

I. I. Shevchenko\*

Pulkovo Observatory of the Russian Academy of Sciences

Pulkovskoje ave. 65/1, St.Petersburg 196140, Russia

## Abstract

Three major properties of the chaotic dynamics of the standard map, namely, the measure  $\mu$  of the main connected chaotic domain, the maximum Lyapunov exponent  $L$  of the motion in this domain, and the dynamical entropy  $h = \mu L$  are studied as functions of the stochasticity parameter  $K$ . The perturbations of the domain due to emergence and disintegration of islands of stability, upon small variations of  $K$ , are considered in particular. By means of extensive numerical experiments, it is shown that these perturbations are isentropic (at least approximately). In other words, the dynamical entropy does not fluctuate, while local jumps in  $\mu$  and  $L$  are significant.

Key words: Lyapunov exponents, Hamiltonian dynamics, chaotic dynamics, standard map.

---

\*E-mail: iis@gao.spb.ru

The standard map is an important object of studies in nonlinear dynamics, mainly because it describes local behaviour of the separatrix map, in a wide range of values of parameters [1, 2]. The separatrix map represents the motion in the vicinity of the separatrices of a nonlinear resonance subject to periodic perturbation [1]–[4]. General properties of the standard map, often in interrelation with those of the separatrix map, were considered and studied in detail in [1]–[9] and many other works. Apart from its relation to the separatrix map, the standard map serves as an important independent mechanical and physical paradigm [5, 7].

Nonlinear resonances are ubiquitous in the problems of modern mechanics and physics. Under general conditions (see [3, 2, 4]), the model of a nonlinear resonance is provided by the nonlinear pendulum with periodic perturbations. Chirikov [3, 2] derived the separatrix map describing the motion in the vicinity of the separatrices of a nonlinear resonance in the perturbed pendulum model. Convenient equations for the map, used e. g. in [10, 11], are the following:

$$\begin{aligned} y_{i+1} &= y_i + \sin x_i, \\ x_{i+1} &= x_i - \lambda \ln |y_{i+1}| + c \pmod{2\pi}, \end{aligned} \tag{1}$$

where  $x, y$  are dynamical variables,  $\lambda$  and  $c$  are constant parameters.

The standard map is the linearization of the separatrix map in the action-like variable  $y$  near a fixed point. The map is given by the equations

$$\begin{aligned} y_{i+1} &= y_i + K \sin x_i \pmod{2\pi}, \\ x_{i+1} &= x_i + y_{i+1} \pmod{2\pi}, \end{aligned} \tag{2}$$

where  $K$  is the so-called stochasticity parameter [1, 2]. On the other hand, the motion near the separatrices of the resonances of the standard map is described by the separatrix map. Therefore major properties of the separatrix map are inherently determined by the properties of the standard map, and vice versa.

In such a way basic properties of the standard map determine the chaotic behaviour near separatrices of a nonlinear resonance. To elucidate these properties is the major goal of the present study.

The calculation of the Lyapunov characteristic exponents (LCEs) is one of the most important tools in the study of the chaotic motion. The LCEs

characterize the rate of divergence of trajectories close to each other in phase space. A nonzero LCE indicates chaotic character of motion, while the maximum LCE equal to zero is a signature of regular (periodic or quasi-periodic) motion. The quantity reciprocal to the maximum LCE characterizes the predictability time of the motion.

Let us consider two trajectories close to each other in phase space. One of them we shall refer to as *guiding* and the other as *shadow*. Let  $d(t_0)$  be the length of the displacement vector directed from the guiding trajectory to the shadow one at an initial moment  $t = t_0$ . The LCE is defined by the formula [4]:

$$L = \limsup_{\substack{t \rightarrow \infty \\ d(t_0) \rightarrow 0}} \frac{1}{t - t_0} \ln \frac{d(t)}{d(t_0)} .$$

The LCEs are closely related to the dynamical entropy [12, 13]. For the Hamiltonian systems with 3/2 and 2 degrees of freedom, Benettin *et al.* proposed the relation  $h = \mu L$  [13, Eq. (6)], where  $h$  is the dynamical entropy,  $\mu$  is the relative measure of the connected chaotic domain where the motion takes place,  $L$  is the maximum LCE of the motion. This formula is approximate. Benettin *et al.* [13] applied it in a study of the chaotic motion of the Hénon–Heiles system.

In what follows, we present numerical data on the chaotic domain measure  $\mu$ , the maximum LCE  $L$ , and their product  $h$  for the standard map. A traditional “one trajectory method” (OTM) has been used for calculation of  $\mu$ . It consists in computing the number of cells explored by a single trajectory on a grid exposed on phase plane. A strict but computationally much more expensive approach for measuring  $\mu$  consists in calculating the values of the coarse-grained area of the chaotic component for a set of various resolutions of the grid, in order to find the asymptotic value of  $\mu$  at the infinitely fine resolution (see [14]). However, a good correspondence of our results on the measure of small regular islands with independent theoretical inferences (see below) verifies that the resolutions we use are already fine enough for the accurate determination of  $\mu$ . A “current LCE segregation method” (CLSM) has been employed in some cases for verification of the obtained values of  $\mu$ . It is based on an analysis of the differential distribution of the computed values of the Lyapunov exponents (current LCEs) of a set of trajectories with the starting values generated randomly or on a regular grid on phase plane. The OTM and CLSM were both proposed and used by Chirikov [1, 2]

in computations of  $\mu$  for the standard map. Analogous methods were used in [15] in computations of the chaotic domain measure in the Hénon–Heiles problem.

Fig. 1 presents our numerical results on  $\mu(K)$ ,  $L(K)$ , and  $h(K)$  at  $K \in [0.5, 1]$ . Fig.1a illustrates discontinuity of the obtained  $\mu(K)$  function. The OTM has been used for constructing this plot; the grid is  $2000 \times 2000$  pixels on phase plane  $(x, y) \in [0, 2\pi] \times [0, 2\pi]$ . The map has been iterated  $n_{it} = 10^8$  times at each value of  $K$ ; the step in  $K$  is equal to 0.001.

$L$  is the maximum Lyapunov exponent of the motion in the main chaotic domain;  $h = \mu L$ . Each value of  $L$  presented in Fig.1b has been computed simultaneously with  $\mu$  for the same trajectory. Everywhere in this work the presented values of the maximum LCEs have been computed by the tangent map method described e. g. in [1, 2].

As follows from Fig.1b, the dynamical entropy  $h = \mu L$  appears to be sharply different, as a function, from the co-products  $\mu$  and  $L$ : the dependences  $\mu(K)$  and  $L(K)$  are discontinuous, while their product  $h(K)$ , on the contrary, looks continuous and monotonous.

At moderate values of  $K$  (at approximately  $K < 4$ ), the discontinuities in  $\mu(K)$  and  $L(K)$  are conditioned by the process of absorption of minor chaotic domains by the main chaotic domain, while  $K$  increases; at larger values of  $K$  (at approximately  $K > 4$ ), it is conditioned by the process of birth and disintegration of new regular islands. The most prominent jump of  $\mu(K)$  at  $K \approx 0.9716$  is conditioned by the absorption of the chaotic domain associated with the separatrices of the half-integer resonance.

The thin solid line in Fig.1b depicts a theoretical approximation of the  $h(K)$  dependence. It is given by the function

$$h(K) = AK^{1/2} \exp\left(-\frac{\pi^2}{K^{1/2}}\right) \quad (3)$$

with  $A = 929.6 \pm 4.0$ ; the latter value is obtained by fitting the observed dependence.

Form (3) for the approximating function is derived in the following way. The maximum mutual divergence of the branches of the splitted separatrix of the integer resonance of map (2) near the point  $x = \pi$  is directly proportional to  $K^{-1/2} \exp(-\pi^2 K^{-1/2})$ ; this relation follows from Eqs. (1.14) and (1.15) in [16]. The divergence of the separatrices characterizes the width of the chaotic layer, and, therefore, the total measure  $\mu$  of the chaotic domain.

On the other hand, the maximum LCE in the domain is on the average directly proportional to  $K$  (see Fig.1c). This has a theoretical explanation. Let us proceed from the relation  $L = L_{sm}/T$ , where  $L_{sm}$  is the maximum LCE of the separatrix map describing the motion, and  $T$  is the average half-period of phase oscillations in the chaotic layer. The quantity  $L_{sm}$  is given by Eq. (12) in [17]:  $L_{sm} \propto \lambda/(1+2\lambda)$ , i. e. it is practically constant at high values of the separatrix map parameter  $\lambda$ . For the standard map,  $\lambda = 2\pi K^{-1/2}$  [1, 2], and therefore  $\lambda > 2\pi$  at  $K < 1$ . The quantity  $T$  is directly proportional to  $K^{-1}$  at small enough values of  $K$  (see Eq. (2.16) in [1], or Eq. (6.18) in [2]). Hence,  $L \propto K$  at small enough values of  $K$ .

The product of  $\mu \propto K^{-1/2} \exp(-\pi^2 K^{-1/2})$  and  $L \propto K$  gives function (3). A paradoxical situation here is that we use formulas for  $\mu(K)$  and  $L(K)$  that are inherently approximate due to the discontinuous nature of these two functions, to obtain a formula for a quantity which might be not discontinuous ( $h(K)$ ), and which may have a smooth analytical representation. Maybe a future theory will allow to derive such representation directly, without appealing to the discontinuous co-products.

In Fig.1c the dependence  $L(K)$  is presented with very fine resolution in  $K$  (the step in  $K$  is 0.0001) at  $K \in [0.1, 1]$ . A larger number of iterations is necessary for saturation of current LCE values at smaller values of  $K$ ; therefore, at  $K < 0.35$  each value of  $L$  presented in Fig.1c has been computed for a single trajectory with  $n_{it} = 5 \cdot 10^8$ , while at  $K \geq 0.35$  the former value  $n_{it} = 10^8$  has been adopted. The saturation at smallest values of  $K$  was checked by recomputing the data at  $K \in [0.10, 0.11]$  with  $n_{it} = 10^9$ .

A self-similar wave-like structure seen in the graph in Fig.1c is due to the absorption of the chaotic layers of integer marginal resonances by the main chaotic domain on increasing the stochasticity parameter  $K$ ; on marginal resonances, see [11].

The downward spikes seen in the  $L(K)$  dependence in Figs. 1b and 1c represent a manifestation of the so-called “stickiness effect” immanent to the chaotic Hamiltonian dynamics in conditions of divided phase space [18]: a chaotic trajectory may stick for a long time to the borders of the chaotic domain, where the motion is close to regular, and therefore the local LCEs are small. Since the computation time is always finite, the stickiness effect, in the case of deep stickings, leads to underestimation of the LCE values; see discussion in [18]. The spikes are especially pronounced, due to the high resolution, in Fig.1c. Spikes due to stickings can be also seen in Figs. 2, 3b

and 4b. It is important to note that these negative jumps in  $L$  represent merely statistical phenomena affecting single trajectories. These jumps are not connected to any perturbations of the chaotic domain measure, contrary to the positive jumps discussed below.

In Fig.2, the dependences  $L(K)$  and  $h(K)$  are presented in a wider range:  $K \in [0, 10]$ . The values of  $\mu$  and  $L$  have been computed simultaneously for a single trajectory taking  $n_{it} = 10^7$ . For computing  $\mu$ , the OTM has been used with the grid  $1000 \times 1000$  pixels on phase plane  $(x, y) \in [0, 2\pi] \times [0, 2\pi]$ . The step in  $K$  is 0.01.

The irregularities present in the  $L(K)$  dependence are apparently smoothed out in the  $h(K)$  graph, in the broad range of  $K$ .

The function

$$h(K) = \ln \frac{K}{2} \quad (4)$$

is depicted in the same Fig.2 (as well as in Figs. 3b and 4b below). This is the well-known logarithmic law derived by Chirikov [1, 2] analytically by means of averaging the largest eigenvalue of the tangent map in assumption that the relative measure of the regular component is small. The presented numerical data indicates (see Fig.2; as well as Figs. 3b and 4b below) that the high- $K$  asymptote of the  $h(K)$  dependence is described by the approximating function

$$h(K) = \ln \frac{K}{2} + \frac{1}{K^2}, \quad (5)$$

instead of Eq. (4). In other words, the asymptote contains a power-law component, in addition to the well-known logarithmic one. The same is valid for the  $L(K)$  dependence, if one ignores the small (and local in  $K$ ) distortions of the function due to the accelerator modes and periodic solutions of higher orders.

The  $\mu(K)$  dependence at large  $K$  (at  $K$  approximately greater than 6) is the horizontal line  $\mu = 1$  with periodic sequences of narrow minima of small and decreasing depth. The most prominent of these sequences correspond to the accelerator modes (emerging at  $K \approx 2\pi m$ ;  $m = 1, 2, \dots$ ) and the 4-periodic solutions (emerging at  $K \approx 2\pi \left(m + \frac{1}{2}\right)$ ;  $m = 1, 2, \dots$ ). The less pronounced sequences of minima correspond to periodic solutions of higher orders.

The local minima in  $\mu(K)$  correspond to local maxima in  $L(K)$ . The discontinuous patterns in  $L(K)$  are removed by the procedure of multiplication of  $L$  by  $\mu$ . Figs. 3a and 3b illustrate the removal of a pattern (a jump) in  $L(K)$  at a high value of  $K$  by means of plotting of  $h = \mu L$  instead of  $L$ . The pattern is conditioned by birth and decay of the islands due to a 4-periodic solution. Figs. 4a and 4b show  $\mu(K)$ ,  $L(K)$ , and  $h(K)$  for a perturbation due to an accelerator mode.

The OTM has been used for computation of  $\mu(K)$  in both Figs. 3a and 4a; the grid is  $2000 \times 2000$  pixels,  $n_{it} = 10^8$ . Each value of  $L(K)$  has been computed for a single trajectory simultaneously with  $\mu(K)$ . The step in  $K$  is  $\Delta K = 0.001$ .

The minimum values of  $\mu$  for the both cases of the accelerator mode and the 4-periodic solution (the minima seen in Figs. 3a and 4a) are in a good agreement with the semi-analytical scaling  $\mu_{reg} = 0.38K_m^{-2}$  derived by Chirikov [5] (see also [1, 2]) for the maximum area of the accelerator mode islands; here  $K_m$  are the values of  $K$  at which the maximum values of area of the regular islands are achieved. The difference is within  $(1 \div 2) \cdot 10^{-4}$  in the both cases. This agreement verifies good accuracy of our measurements of  $\mu$ .

Note that the inversely quadratic decay of area of the regular islands emerging at  $K \approx \pi m$ ;  $m = 2, 3, \dots$ , i. e. for the both cases of the accelerator modes and the 4-periodic solutions, was recently rigorously derived by Giorgilli and Lazutkin [9]. They refer to an unpublished work by Lazutkin, Petrova, and Svanidze for the numerical confirmation of this theoretical result.

In the both cases of Figs. 3 and 4, the patterns in  $L(K)$  are substantially eliminated by considering  $h$  instead of  $L$ . What is the mechanism for the “maximum LCE—chaos measure” local anticorrelations?

Let us consider an island’s decay. The small self-similar variations of  $\mu(K)$  and  $L(K)$  during the decay are due to the absorption (by the main chaotic domain) of the chaotic layers of the chains of islands separating from the main island’s border on increasing  $K$ . We mark the properties of the whole chaotic domain just before and after an act of the absorption by the subscripts  $b$  and  $a$  respectively. Assume that the absorbed layer has almost zero local value of the maximum LCE. Then, the global value of the maximum LCE after an act of the absorption is the value averaged over the whole accessible area:  $L_a = (L_b\mu_b + 0 \cdot \delta\mu)/(\mu_b + \delta\mu)$ , where  $\delta\mu$  is the measure of the layer absorbed,  $\mu_b$  and  $L_b$  are the value of the measure of the main connected chaotic domain

and the value of the maximum LCE of the motion in this domain before the act of the absorption. Then, the new value of the dynamical entropy  $h_a = \mu_a L_a = (\mu_b + \delta\mu)(\mu_b L_b / (\mu_b + \delta\mu)) = \mu_b L_b$  remains equal to the old one  $h_b$ , i. e.  $h(K)$  is insensitive to such absorptions and is subject solely to “secular” variation.

This reasoning explains also the smoothing out of the  $h(K)$  dependence at  $K < 1$ , since the growth of the main chaotic domain at these values of  $K$  is conditioned just by the absorption of the external chaotic layers.

However, this reasoning is not completely satisfactory in the both cases, because whatever small the local Lyapunov exponent in the absorbed layer might be, it is not strictly zero. Besides, Fig. 3a clearly demonstrates that the process of the consequent absorptions of the layers takes place during the decay of the pattern, but not during its growth: contrary to a fractal (due to the absorptions) structure of the  $\mu(K)$  dependence during the decay, this dependence is apparently smooth, of course up to the accuracy of our graph, during the growth. So, the approximate conservation of the dynamical entropy is probably not due to the just described mechanism at intervals of  $K$  corresponding to the growth of islands. In fact, the largest visible deviations (though small) from the conservation occur at the intervals of growth. Due to the smallness of these deviations, it is not clear currently whether they are real, or the adopted resolution of our numerical experiments is insufficient.

Apart from the need for a complete theoretical explanation in the considered case of the standard map, an important problem is whether the perturbations due to the emergence and disintegration of islands of stability in chaotic domains are isentropic, at least approximately, in any Hamiltonian system. A hint for an affirmative answer at least in case of a particular system with two degrees of freedom can be found in [15]: indeed, the energy dependence of the dynamical entropy of the chaotic domain in phase space of the Hénon–Heiles system (Fig.8 of that paper) is more regular, or smoothed out, in comparison with the corresponding energy dependence of the maximum LCE (Fig. 2 of that paper).

Of course, if the system can be approximated locally by the standard map, the perturbations of the local chaotic behaviour, according to our numerical results, should be approximately isentropic.

Let us summarize the main results. The measure  $\mu$  of the main connected chaotic domain of the standard map, the maximum Lyapunov exponent  $L$  of the motion in this domain, and the dynamical entropy  $h = \mu L$  have been studied as functions of the stochasticity parameter  $K$  by means of extensive



numerical experiments. It has been found that the  $h(K)$  dependence behaves like a continuous and monotonous function (up to the experimental accuracy, of course), while the  $\mu(K)$  and  $L(K)$  functions are discontinuous. A semi-analytical approximating relation for the dynamical entropy at  $K < 1$  has been derived.

It has been shown that the process (upon small variations of  $K$ ) of birth and disintegration of the islands of stability inside the chaotic domain does not result in fluctuations of the dynamical entropy  $h(K)$  (while  $\mu(K)$  and  $L(K)$  fluctuate); i. e. these perturbations are isentropic, at least approximately. A tentative explanation of the isentropic behaviour has been given.

The author is thankful to B. V. Chirikov for valuable discussions. This work was supported by the Russian Foundation for Basic Research (project number 03-02-17356).

## References

- [1] B. V. Chirikov, Interaction of Nonlinear Resonances (Novosib. Gos. Univ., Novosibirsk, 1978) [in Russian].
- [2] B. V. Chirikov, Phys. Rep. 52 (1979) 263.
- [3] B. V. Chirikov, Nonlinear Resonance (Novosib. Gos. Univ., Novosibirsk, 1977) [in Russian].
- [4] A. J. Lichtenberg and M. A. Lieberman, Regular and Chaotic Dynamics (Springer-Verlag, New York, 1992).
- [5] B. V. Chirikov, Zh. Eksp. Teor. Fiz. 110 (1996) 1174 [JETP 83 (1996) 646].
- [6] B. V. Chirikov and D. L. Shepelyansky, Phys. Rev. Lett. 82 (1999) 528; 89 (2002) 239402-1.
- [7] J. D. Meiss, Phys. Rep. 64 (1992) 795.
- [8] D. V. Treshchev, An Introduction to the Perturbation Theory of Hamiltonian Systems (FAZIS, Moscow, 1998) [in Russian].
- [9] A. Giorgilli and V. F. Lazutkin, Phys. Lett. A 272 (2000) 359.

- [10] B. V. Chirikov and D. L. Shepelyansky, *Physica D* 13 (1984) 395.
- [11] I. I. Shevchenko, *Phys. Scr.* 57 (1998) 185.
- [12] Ya. B. Pesin, *Doklady Akademii Nauk SSSR* 226 (1976) 774 [in Russian].
- [13] G. Benettin, L. Galgani, and J. M. Strelcyn, *Phys. Rev. A* 14 (1976) 2338.
- [14] D. K. Umberger and J. D. Farmer, *Phys. Rev. Letters* 55 (1985) 661.
- [15] I. I. Shevchenko and A. V. Melnikov, *Pis'ma Zh. Eksp. Teor. Fiz.* 77 (2003) 772 [*JETP Letters* 77 (2003) 642].
- [16] V. V. Vecheslavov and B. V. Chirikov, *Zh. Eksp. Teor. Fiz.* 114 (1998) 1516 [in Russian].
- [17] I. I. Shevchenko, *Kosmich. Issled.* 40 (2002) 317 [*Cosmic Res.* 40 (2002) 296].
- [18] I. I. Shevchenko, *Phys. Lett. A* 241 (1998) 53.

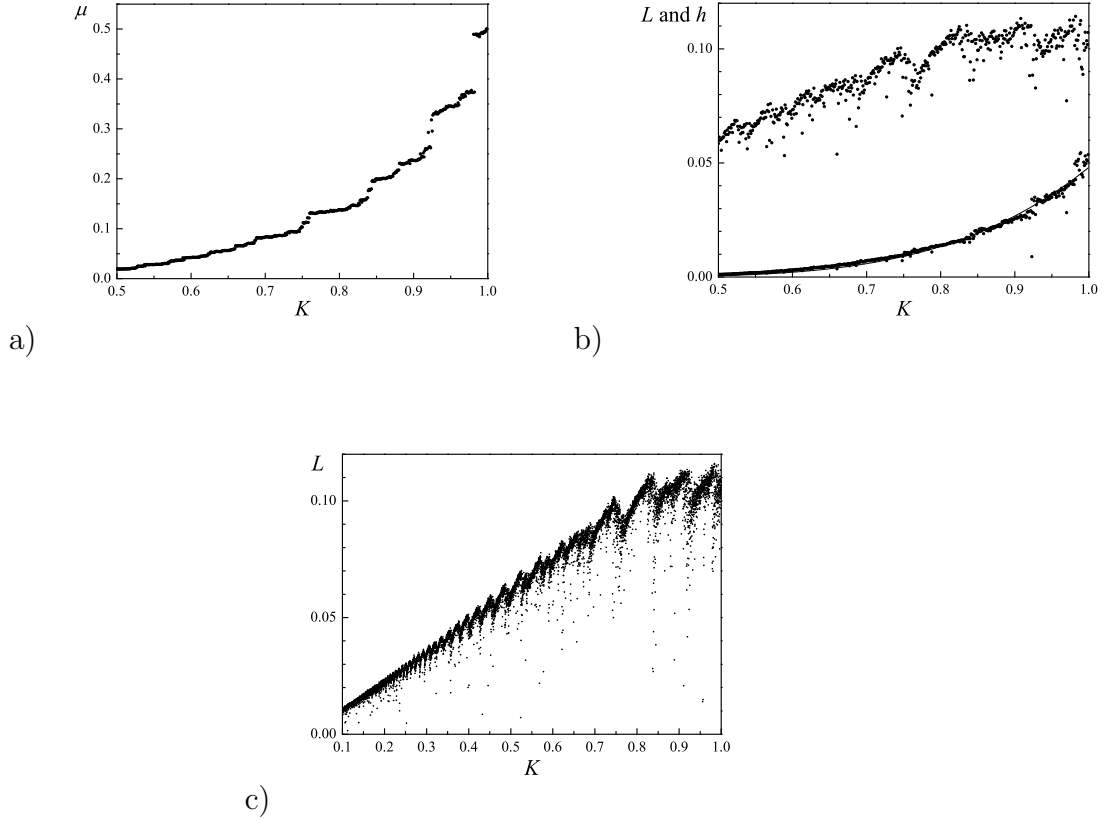


Figure 1: The  $\mu(K)$  dependence at  $K < 1$  (a);  $L(K)$ ,  $h(K) = \mu(K)L(K)$ , and the theoretical curve for  $h(K)$  given by Eq. (3) (the thin solid line) (b);  $L(K)$  in a higher resolution (c).

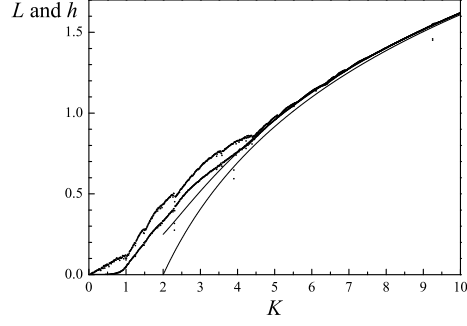


Figure 2:  $L(K)$  (the upper curve) and  $h(K)$  in a wider range of  $K$ . The thin solid lines are given by Eqs. (4, 5).

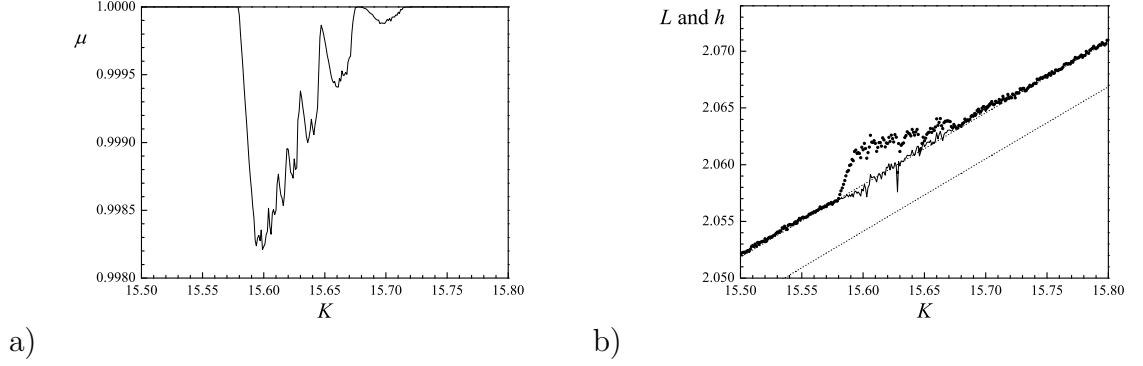


Figure 3: The  $\mu(K)$  dependence for a pattern at  $K \approx 15.6$  due to a 4-periodic solution (a);  $L(K)$  and  $h(K)$ , drawn by bold dots and solid curve respectively, for the same pattern (b). The thin dotted lines are the same as the thin solid lines in Fig. 2.

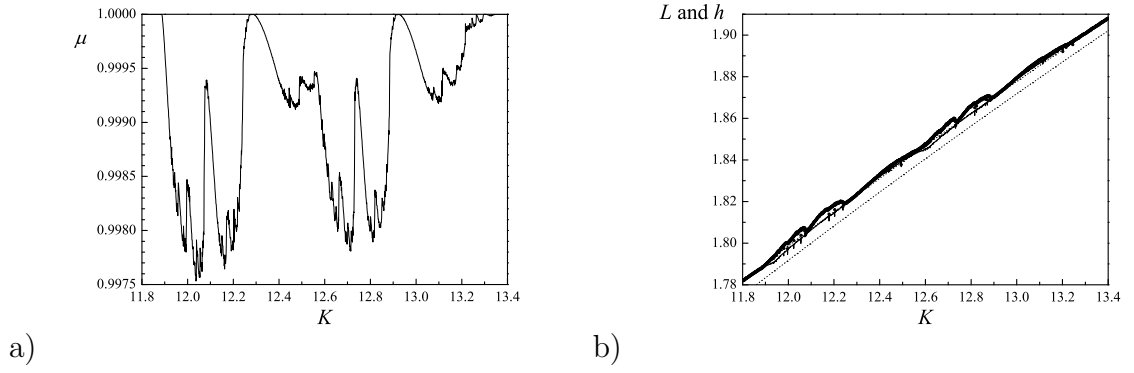


Figure 4: The  $\mu(K)$  dependence for a pattern at  $K \approx 12 \div 13$  due to an accelerator mode (a);  $L(K)$  and  $h(K)$  for the same pattern (b). The thin dotted lines are the same as the thin solid lines in Fig. 2.